GMD

Practical Trade-offs in Robust Target Following

Christfried Webers & Uwe R. Zimmer

GMD - Japan Research Laboratory
AIM Building 8F, 3-8-1, Asano, Kokurakita-ku
Kitakyushu-city, 802-0001, Japan
{christfried.webers | uwe.zimmer}@gmd.gr.jp

This article discusses two Lyapunov based robust target following techniques and introduces a method based on the superposition of elementary vehicle dynamics. All three approaches are discussed and physically tested together with a known Lyapunov method for closed loop control. Emphasis is given on the discussion of distinguishing features and parameters relevant for practical selection of target following methods, where manoeuvring space, velocities and accelerations are strictly limited. Uncertain position information and limitations in accuracy and available computational power are especially considered. All discussed results are measured in physical experiments.

1. Motivation

A common task in mobile robotics is to drive a robot to a certain position and orientation as fast as possible and within the limits of the static and dynamic properties of the robot setup. Autonomous robots may not only choose targets which are not smoothly connected, but also the choice itself may not be predictable any more. Therefore a robust behaviour in reaching a noisy, drifting, or even stochastically moving target is a necessary condition for successful applications with autonomous robots. In physical setups, where the position of the target can only be determined approximately and disturbances are unavoidable, there is no principal difference between posing and target following. Continuous corruptions and corrections in the position measurement appear on the motion control level in the same way as a purposefully moved target. Robust posing control represents thus always also a target following system.

For nonholonomic systems (which are the majority of current mobile robots), a theorem by Brockett [3] shows that stabilization by time-invariant smooth state feedback is not possible.

Several approaches, among them time-varying [8] and discontinuous [1][2] have been proposed to solve the posing or more general the target following problem. For a detailed discussion see e.g. [6][7].

In this paper, three approaches are discussed and tested in experiments:

- a Lyapunov based approach in which the velocity is proportional to the distance.

- a Lyapunov based approach in which the velocity is bounded.

- an approach where the dynamics of three distinct situations (far from, orienting towards and converging into the goal) are modelled and superimposed, resulting in one smooth feedback law.

The sensor readings in the experiments have been additionally (artificially) disturbed in order to prove the robustness of the discussed methods.

2. The kinematic model and physical constraints

The model, describing the motion of the cartesian unicycle vehicle is given by

$$
\begin{aligned}
\dot{x} &= u\cos\phi \\
\dot{y} &= u\sin\phi \\
\dot{\phi} &= \omega
\end{aligned}
\tag{1}
$$

being u the linear velocity in the direction of ϕ and ω the angular velocity (figure 1).

In this article, the point-to-point navigation task is considered, i.e. the vehicle starts at point (x_S, y_S) with heading ϕ_S and should be driven with appropriate u and ω to the goal. Without loss of generality the goal can be chosen to be $(x_G, y_G, \phi_G) = (0, 0, 0)$.

Furthermore, u and ω should not explicitly depend on the time but only on the state variables thereby leading to autonomous differential equations for the state variables.

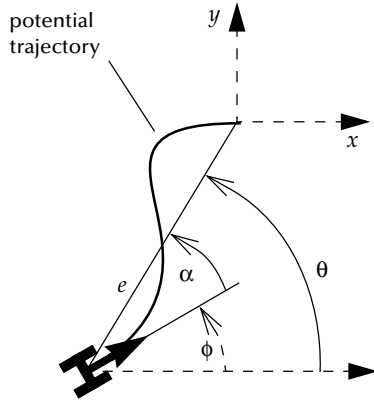Brockett's Theorem [3] shows that the stabilization for the system (1) can not be solved, because the

figure 1 : Unicycle kinematic model

number of dimensions spanned by linearly independent vectors is not equal to the number of controls.

On the other hand, if the state itself is not defined at the equilibrium, Brockett's Theorem does not prevent the stabilization. This can be achieved by a nonlinear coordinate transformation.

A suitable choice for this transformation are the following coordinates which were introduced in [1]

$$
\begin{aligned}
e &= \sqrt{x^2 + y^2} \\
\theta &= \operatorname{atanh}(-y, -x) \\
\alpha &= \theta - \phi
\end{aligned}
\tag{2}
$$

being $\operatorname{atanh}(y, x) \in (-\pi, \pi]$ the four quadrant inverse tangent function describing the angle between a line from $(0,0)$ to (x,y) and the positive x-axis.

With the new coordinates e, α, θ the kinematic model (1) is transformed to (3), on which our further considerations will be based on:

$$
\begin{aligned}
\dot{e} &= -u \cos \alpha \\
\dot{\theta} &= \frac{u \sin \alpha}{e} \\
\dot{\alpha} &= -\omega + \frac{u \sin \alpha}{e}
\end{aligned}
\tag{3}
$$

Any real vehicle has limitations which depend on the vehicle itself or on its interaction with the environment. The following ones are considered here:

a. bounded linear velocity $|u| \leq u_{max}$

b. bounded angular velocity $|\omega| \leq \omega_{max}$

Normally, the low level motor controllers prevent any dangerous settings of the controls which would break the gears of the vehicle. A more serious problem is the use of control setting ranges which can not be physically realized in the vehicle and would result in an invalid experimental setup.

c. bounded lateral acceleration $a = |u \cdot \omega| \leq a_{max}$

Path tracking experiments depend on the precision of the odometry. If in a curve the lateral acceleration of the vehicle is to strong, the wheels loose close contact to the ground and the odometry data will no longer be meaningful.

d. bounded curvature $c = \left| \dfrac{\omega}{u} \right| \leq c_{max}$

Additionally to the above stated restrictions which apply to every vehicle, a large class of vehicles can not turn on the spot, i.e. the curvature is bounded.

e. only forward moving vehicles $u \geq 0$

Moving is assumed to be possible in one direction only in order to avoid additional bifurcations.

3. Linear velocity Lyapunov approach (LV)

In [1] and [4] it was shown that with the assumption

$$
u = \gamma e \qquad \gamma > 0
\tag{4}
$$

for the linear velocity and

$$
\begin{aligned}
V &= \frac{1}{2}(\alpha^2 + h\theta^2) \qquad h > 0 \\
\dot{V} &= -\gamma \beta \alpha^2 \qquad \beta > 0
\end{aligned}
\tag{5}
$$

for the Lyapunov function and its derivative a nonlinear, time-invariant, globally and asymptotically converging control law for ω of the form

$$
\omega = \gamma \left(\sin \alpha + \frac{h \theta \sin \alpha}{\alpha} + \beta \alpha \right)
\tag{6}
$$

$$
1 < h \; ; \; 2 < \beta < 1 + h
$$

can be found.

Note, that a Lyapunov function in the strict sense would mean, that also the state at $e = 0$ is defined and reachable. But the nonlinear transformation (2) was introduced exactly to avoid a defined state at $e = 0$ in order to circumvent Brocketts Theorem [3]. Therefore, the existence of a Lyapunov function is assumed in every vicinity of $e = 0$ only.

With (4) and (6) the curvature $c = \omega/u$ will be indirect proportional to e. And because ω does not depend on the distance e solutions for the same starting angles α, θ but different e will be similar to each other. This scaling property is the reason why this approach needs a large space around the goal in both dimensions as can be seen from figure 2.

Assumption (4) can not be realized on a vehicle because one would get to big velocities or one would have to set γ to a very small value resulting in a very slow motion. Therefore, u will be bounded to u_{max}. It can be shown, that convergence can be guaranteed

if in addition to the conditions (6) the parameter β is to be chosen

$$\beta \geq \frac{4e_S}{3\pi^2} \tag{7}$$

where e_S is the initial distance from the goal.

4. Bounded velocity Lyapunov approach (BV)

While (4) introduced the velocity to depend linearly on the distance, the following assumption for the velocity

$$u = u_{max}\tanh(\kappa e) \tag{8}$$

establishes the existence of an upper bound for the velocity in the Lyapunov approach. Here, κ is a measure for the deceleration of the vehicle when it approaches the goal.

With the same Lyapunov function (5) the angular velocity becomes

$$\omega = u_{max}\left(\frac{\tanh(\kappa e)\sin\alpha}{e} + \right. \tag{9}$$
$$\left. \frac{h\theta\tanh(\kappa e)\sin\alpha}{\alpha e} + \beta\alpha\right)$$

Compared to LV this approach does no longer lead to an ω which is independent of the distance from the goal e. Instead, for large distances, ω is proportional to the angle α thus resulting in a faster turn to the goal if the vehicle is currently heading away from the goal. The resulting curve is closer to the x-axis than the curve in LV.

For the approach to the goal, the behaviour of the solutions for $(e, \theta, \alpha) \rightarrow (0, 0, 0)$ must be analysed. The approximation of the state equations (3) with u and ω from (8) and (9) provide the linearized state equations

$$\dot{e} = -u_{max}\kappa e \tag{10}$$

and

$$\begin{pmatrix} \dot{\alpha} \\ \dot{\theta} \end{pmatrix} = \begin{bmatrix} -\beta u_{max} & -h\kappa u_{max} \\ \kappa u_{max} & 0 \end{bmatrix} \begin{pmatrix} \alpha \\ \theta \end{pmatrix} \tag{11}$$

The eigenvalues of the matrix in (11) can then be found as

$$\lambda_{1,2} = \frac{u_{max}}{2}(-\beta \pm \sqrt{\beta^2 - 4h\kappa^2}) \tag{12}$$

In order to reach the target on a straight line no oscillations are allowed ($\beta^2 - 4h\kappa^2 > 0$). Also, the angles (θ, α) must approach zero faster then e. This can be guaranteed if the dominant eigenvalue of (12) is strictly greater than the factor governing the decrease of e in (10).

$$u_{max}\kappa < \frac{u_{max}}{2}(\beta - \sqrt{\beta^2 - 4h\kappa^2}) \tag{13}$$

This provides us the conditions for the convergence

$$1 < h \; ; \; 2\sqrt{h}\kappa < \beta < (1 + h)\kappa \tag{14}$$

of the bounded velocity approach.

Although the velocity is bounded, this approach does not provide adequate bounds for the angular velocity ω, the lateral acceleration and the curvature. Therefore, in practical experiments the bounds will be enforced by reducing u and ω accordingly. This allows for driving the vehicle with maximum velocities while keeping within the robot's physical limitations. In principle, the same procedure could be employed for LV also.

Further work should include the bounds on the lateral acceleration and the curvature into the Lyapunov approach. This would mean to introduce a dependence of the velocity u from ω in (8) because it is obvious that the linear velocity of the vehicle should be at its maximum when the vehicle is moving on a straight line, while it should be reduced for curves in order to keep the lateral acceleration bounded.

5. Superimposed Dynamics (SD)

The following approach could be sketched as a superposition of dynamics, where the following aspects are considered and can be formulated individually (e, α, ϕ as introduced above) in the first place:

- *Approaching the goal directly*:
  Far from the goal, only the difference in the heading towards the goal α is considered to control the vehicle with:

$$\omega = \omega_{max}\tanh\left(\frac{c_w\alpha}{\omega_{max}}\right) \tag{15}$$

$$u = u_{max}(u_{min} + (1 - u_{min})_{max}\{0, \cos\alpha\}^{c_l}) \tag{16}$$

- *Approaching the goal with specific orientation*:
  Closer to the goal, the trajectory needs to consider the difference to the requested final orientation ϕ as well as the distance to the goal e with:

$$\delta_{close} = c_m\frac{\pi}{2}\tanh\left(\frac{\alpha + \phi}{1 - c_m}\right) \tag{17}$$

approximating the direction to a point on the negative x-axis in distance $c_m e$ from the goal, which would be precisely for $|\alpha| < \pi/2$:

$$atan\left(\frac{c_m\sin\alpha}{1 - c_m\cos\alpha}\right) \tag{18}$$

The derived control equations are:

$$\omega = \omega_{max}\tanh\left(\frac{c_\omega(\delta_{close} + \alpha)}{\omega_{max}}\right) \tag{19}$$

$$u = u_{max}\tanh(ec_b) \tag{20}$$

- *At the goal*:
  When so close to the goal that the uncertainties in

the positioning are of the same dimension than the actual remaining distance, the direction to the goal is no longer influencing the dynamics. This is especially important, if large changes in α (which are unavoidably increasing as the goal gets closer) should not lead to arbitrary large changes and thus instabilities in ω. Thus the control laws at the goal consider ϕ and e only:

$$\omega = \omega_{max}\tanh\left(\frac{-c_\omega\phi}{\omega_{max}}\right) \quad (21)$$

$$u = u_{max}\tanh(ec_b) \quad (22)$$

Note that these final approach strategy is *not* reaching the goal exactly, but offers a stable way to get close to the goal only.

By superimposing these aspects of the control task, a closed representation can be formulated, where the robustness of the simple individual parts are preserved. A related method, superimposing dynamics separated in activation and target dynamics can be found in [5].

First the currently required deviation δ from the direct heading to the goal is expressed with:

$$\delta = c_m\frac{\pi}{4}\tanh\left(\frac{\alpha+\phi}{1-c_m}\right)\cdot(1-\tanh(c_s(e-c_d))) \quad (23)$$

where c_m gives the strength which attracts the vehicle to a straight line into the goal (i.e. the smoothness or precision of the trajectory can be controlled here), c_d sets the distance at which the intended goal orientation is started to be considered, and c_s gives the speed of the transition from 'straight towards the goal' to the 'final approach' behaviour.

Second the linear velocity reduction and the transition to the relaxed 'being there' dynamic of the control can be formulated as:

$$u_{fo} = 1-(\alpha_d(1-\tanh(ec_b))) \quad (24)$$

$$a_{fo} = 1-(\alpha_d(1-(\tanh(ec_a))^6)) \quad (25)$$

where

$$\alpha_d = {}_{max}\{0, \cos((2\alpha/3)^4)\} \quad (26)$$

Finally the closed control laws for ω and u can be defined as:

$$\omega = \omega_{max}\tanh\left(\frac{\omega_{amp}\delta_o}{\omega_{max}}\right) \quad (27)$$

$$u = u_{max}u_{fo}\tanh\left(\frac{a_l}{|\omega|u_{max}}\right) \quad (28)$$

where

$$\delta_o = a_{fo}(\delta+\alpha+\phi)-\phi \quad (29)$$

The parameter a_l determines the tolerated lateral acceleration. Equation (24) and (25) reflect the fact that deceleration and relaxation is only reasonable, when the goal is in front of the vehicle, where c_a and c_b control the angular relaxation and the linear deceler-

ation respectively. The parameter ω_{amp}, u_{max} and ω_{max} are the overall velocity amplifications and limits.

This approach has no singularities (beside the obvious bifurcation, when the goal is exactly behind the vehicle) and can be adjusted according to the physical constraints of the setup directly. The vehicle will be lead only close to the goal considering the uncertainties of the available position information. Therefore instabilities due to overestimations of the position reliability or precision are avoided. Parameters chosen for the physical experiment are:

$$
\begin{array}{llll}
u_{max} = 1.6 & [m/s] & \text{maximal } u & \\
\omega_{max} = 60 & [°/s] & \text{maximal } \omega & \\
\omega_{amp} = 3 & [1/s] & \text{amplification in } \omega & \\
c_a = 10 & [1/m] & \text{angular relaxation} & \\
c_b = 1 & [1/m] & \text{deceleration} & (30) \\
c_m = 0.6 & [0,1] & \text{smoothness of final turn} & \\
c_d = 2 & [m] & \text{starting final approach} & \\
c_s = 0.5 & [1/m] & \text{smoothness of bending away} & \\
a_l = 0.4 & [m/s^2] & \text{max lateral acceleration} &
\end{array}
$$

6. Results

The physical system employed for all experiments offers the following sensor systems and actuators:

- *3-axis gyroscope*: stability: $\approx 1°/s$; sampling frequency: $176\,Hz$.

- 3 *linear accelerometers*: resolution: $5\,mG$; sampling frequency: $176\,Hz$.

- 2 *encoders*: resolution: ≈ 86000 ticks per wheel revolution; sampling frequency: $58\,Hz$

- 4 wheel drive with *differential steering*, a maximal linear speed of $\approx 1.6\,m/s$ and a maximal angular speed of $\approx 150°/s$; control frequency: $193\,Hz$.

Gyroscopes, accelerometers and encoders are combined to stabilize for glitches in the encoders (wheel slip) and drifts in the gyroscopes. Since the robustness of the approaches against uncertainties is to be proven the resulting position measurement is deteriorated by adding $\pm10\,mm/sample$ uniform noise on the linear forward movement and $\pm3°/sample$ uniform noise on the orientation information, as measurement by the encoders.

In order to evaluate the different approaches, the vehicle is requested to approach a goal $5.4\,m$ behind the starting position in the same orientation as it started. In figure 2, the driven paths as recorded by odometry (and projected as a bird's eye view) are plotted, where the starting point is on the right side with the vehicle facing to the right. The constraints are to reach the goal as fast as possible but keep the accelerations and velocities in reasonable limits (tolerated
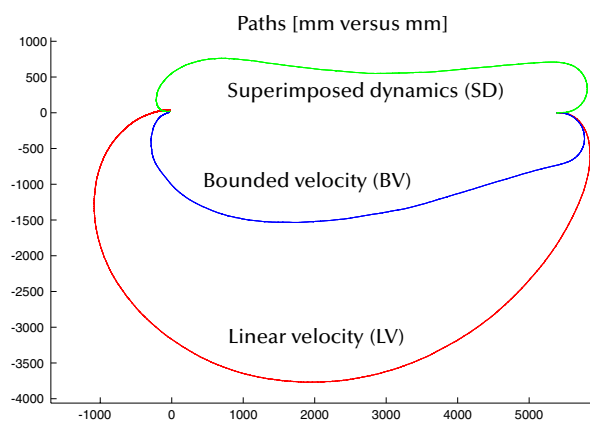
figure 2 : Generated paths

lateral acceleration: $0.4\,m/s^2$; top speed: $1.6\,m/s$ and angular velocity at $110°/s$ at most).

The durations, lateral accelerations, as well as the employed space in *y*, and the maximal curvature needed for reaching the goal within a range of $3\,cm$ and the orientations close to the goal position are:

	total duration	max. lateral acceleration	employed space (*y*)	orientation at goal	maximal curvature
	[s]	[m/s^2]	[mm]	[°]	[$°/m$]
LV:	42.35	0.91	3768	-64.9	2066
BV:	10.95	0.40	1532	6.9	229
SD:	13.00	0.40	709	0.5	526

The maximal curvature along the paths occurs with the LV and BV method at the goal position, where the strongest angular corrections are forced. The curvature of the LV method is not bounded by any means thus the vehicle tries to turn almost on the spot close enough to the goal. Since the curvature of the BV method is bounded explicitly it is still very low, al-
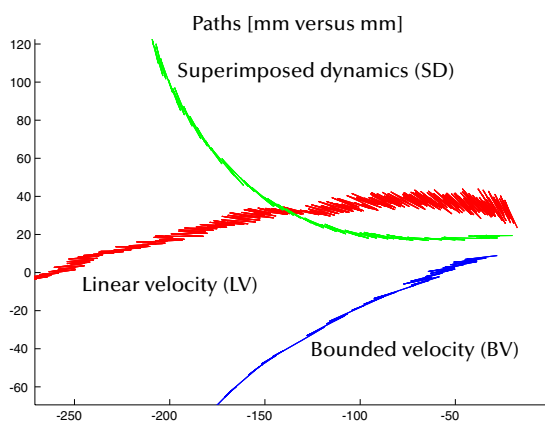

figure 3 : End approaches

lowing for corrections in the borders of the vehicles capabilities only. The maximal curvature in the SD method occurs in the last phase of the path also, but significantly before the goal position, because angular corrections are suppressed closer to the goal. It is not explicitly bounded here, nevertheless the method allows naturally for limited curvature paths only.

A closer look at the final approach phase can be found in figure 3, where strong corrections can be detected in the LV and BV methods trying to reach the goal exactly and turning (in case of LV) the vehicle by 65° off the intended orientation in $29\,mm$ off the goal. In the superimposed dynamics method the vehicles's orientation is controlled to zero before reaching the goal and variations in α are less considered closer to the goal. Therefore the orientation and the overall behaviour can be kept stable until the very end, but convergence to the goal position is not forced.

Due to the high lateral starting acceleration of the LV method the maximal speed needed to be set to 0.5 m/s here (figure 7), which is then constant for most of the path and linearly reduced near the goal. Nevertheless a top lateral acceleration of $0.9\,m/s^2$ needed to be tolerated (figure 4) in order not to disqualify this method with regard to the overall travel duration.

Both other methods keep in the given limit of $0.4\,m/s^2$ (figure 5, 6) and using the tolerated top speed of $1.6\,m/s$ (figure 8, 9). Differences throughout the path are larger variations in omega and lateral acceleration for the BV method, but therefore reaching the goal approximately 2 seconds earlier than the superimposed dynamics method.

All shown methods were executed under realtime constraints with a permanent control frequency of $193\,Hz$. All control laws are one step direct evaluations without any recursions or loops (the computational complexity of all approaches is O(1)) and the actual computation time constant depend on the evaluation of the individually required trigonometric functions only. The O(1) complexity enables this control methods for all hard realtime control tasks.

7. Conclusion

Advantages and drawbacks of principally different control methods have been illustrated. Of course, a single universally applicable control method could not be identified, but the individual features, benefits, and limitations are better understood concerning practical applications, where strict physical, kinematic, and dynamical limitations are a given reality. Future work concentrates on a variety of physical setups, and the development of methods combining especially physically motivated adjustability, convergence under disturbed measurements, and stability in fast moving target environments.

References

[1] M. Aicardi, G. Casalino, A.Bicchi, and A. Balestrino
Closed Loop Steering of Unicycle-like Vehicles via Lyapunov Techniques
IEEE Robotics and Automation Magazine, March 1995, pp. 27-35

[2] A. Astolfi
Discontinuous control of nonholonomic systems
Systems & Control letters, vol. 27, pp. 37-45, 1996

[3] R.W. Brockett, R.S. Millmann, and H.J. Sussmann, eds.
Differential Geometric Control Theory
ch. Asymptotic Stability and Feedback Stabilization, by Brockett, R.W., pp. 181-191. Birkhauser, Boston, USA, 1983

[4] G. Indiveri
Kinematic Time-invariant Control of a 2D Nonholonomic Vehicle
38th Conference on Decision and Control, CDC'99, Phoenix, USA, December 1999.

[5] H. Jaeger
The Dual Dynamics Design Scheme for Behaviour-based Robots: a Tutorial
GMD Technical report #966, St. Augustin, Germany 1996 (23 pp.)

[6] M. Krstić , I. Kanellakopoulos, P. Kokotović
Nonlinear and Adaptive Control Design
John Wiley & Sons, Inc., New York 1995.

[7] J.-P. Laumond (ed.)
Robot Motion Planning and Control
Lecture Notes in Control and information Sciences 229, Springer, 1998.

[8] P. Morin, C. Samson
Time-varying exponential stabilization of a rigid spacecraft with two central tourques
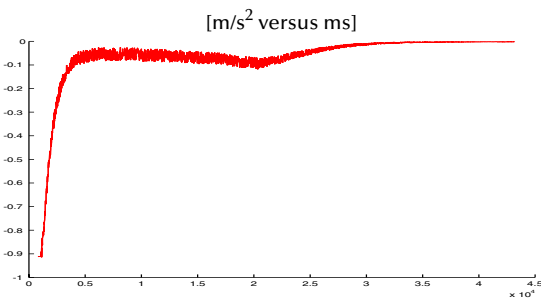IEEE trans. on Automatic control, vol. 42, No. 4, pp. 528-534, 1977

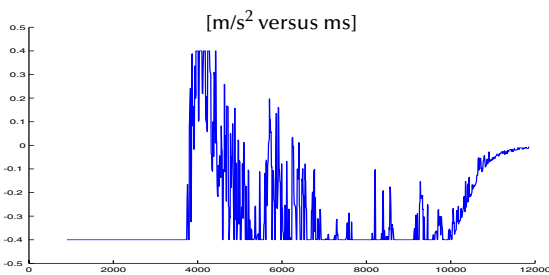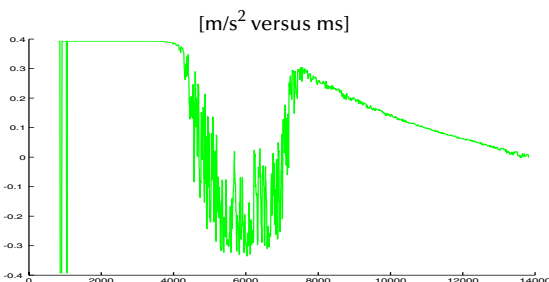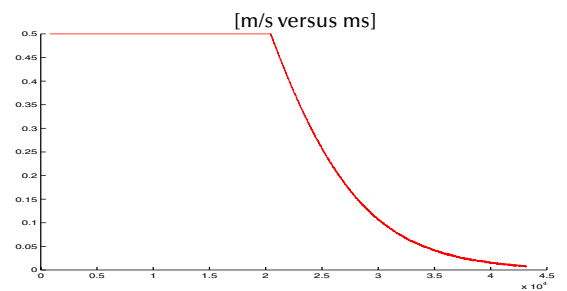*figure 4 :* Lateral acceleration with the LV method

figure 7 : Linear velocity profile with the LV method

figure 5 : Lateral acceleration with the BV method
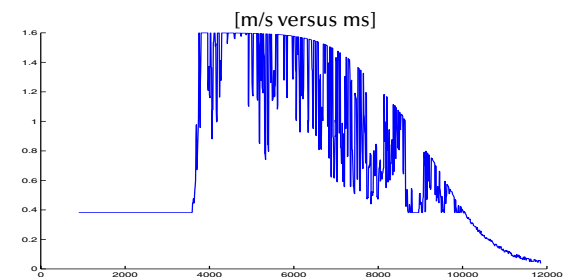
figure 8 : Linear velocity profile with the BV method

figure 6 : Lateral acceleration with the SD method
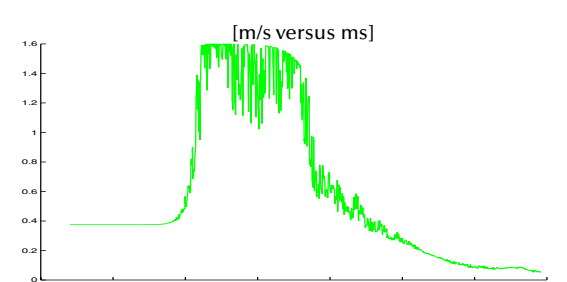
figure 9 : Linear velocity profile with the SD method